JOURNAL OF GUIDANCE, CONTROL, AND DYNAMICS
Vol. 32, No. 4, July–August 2009

Nearly Circular Equatorial Orbits About an Oblate Body with Atmosphere

Mayer Humi*
Worcester Polytechnic Institute, Worcester, Massachusetts 01609
and
Thomas Carter†
Eastern Connecticut State University, Willimantic, Connecticut 06226

DOI: 10.2514/1.40861

This paper studies nearly circular equatorial orbits of satellites in the gravitational field of an oblate body that includes the J_2 term and quadratic drag. We derive analytic expressions for the orbit of a satellite under these conditions even if the local atmospheric density is provided in tabular form. This work includes four distinct atmospheric density models. A closed-form solution of the orbit equation for each model is compared with the numerical integration of the equations of motion with a test model of the atmospheric density, disclosing the accuracy of the analytic solution that follows from each model. For an orbital decay of 900 m over 160 revolutions, the least accurate model revealed an error of 5 m, whereas the most accurate model produced an error of 0.4 m.

I. Introduction

THE search for an analytical approach to orbit determination and relative-motion studies has taken place over many years using various assumptions [1–26]. We list some representative studies of two-body orbits and their related relative motion [2–4,7–10]. Some early studies include the J_2 effect and atmospheric drag [1,6,11,12]. Much of the early work is summarized in the paper by Liu [13]. Some later studies have concentrated on atmospheric drag [14,16,18,19] of a satellite in the gravitational field of a spherical body and drag-free orbits in the gravitational field of an oblate body [20–23,26].

Some of the early work, as summarized by Liu [13], includes atmospheric drag with rotating atmosphere and orbits of arbitrary inclinations about an oblate planet. Other effects are sometimes treated as higher-order perturbations. Typically, a Keplerian solution to the two-body problem is adjusted through a method of variations of constants with approximations found from dominant terms in series expansion. One of the most important of these approaches is found in the work of Brouwer and Hori [11]. They use Delaunay variables, but transform the equations of motion into canonical variables for the drag-free problem. The drag acceleration is expanded in powers of eccentricity and in multiples of the mean anomaly, then integrated. Although the approximating formulas are in analytic form, they are long and cumbersome.

The present work is more restrictive, requiring a stationary atmosphere and orbits that are equatorial and nearly circular initially, but have the advantage that the formulas found are accurate and concise, obtained from simple linear differential equations of second or third order. The atmospheric density function can be quite general: we require data only in tabular form. We build atmospheric density models from these data. Some simulations compare the accuracy of these models with that of numerical integration of the equations of motion with a test atmospheric density function.

The next section presents a derivation of the orbit equation for an equatorial plane and includes J_2 effects and atmospheric drag. This is followed by a section that presents closed-form solutions of the equations of motion for each of the four atmospheric density models, including simulations comparing each with numerical integration using a test atmospheric density model.

II. Equatorial Orbits About an Oblate Body with Drag

In the gravitational potential of an oblate body, the most important correction term is that containing J_2, the coefficient of the primary zonal harmonic. With this term, the gravitational potential of the Earth or other oblate spheroid is given approximately by [5]

$$U = -\frac{\mu}{r}\left[1 - \frac{R^2 J_2}{r^2} P_2(\cos\phi)\right] \tag{1}$$

With this equation, we associate an inertial coordinate system attached to the center of the oblate body. In this system, $\mathbf{r}$ is the radius vector, where $r = |\mathbf{r}|$, ϕ is the colatitude angle, R is the radius of the oblate body in the equatorial plane, μ represents the product of the universal gravitational constant and the mass of the spheroid, and P_2 is the second-order Legendre polynomial. We use a dot above a symbol to denote differentiation with respect to time t (e.g., $\dot{r} = dr/dt$).

The force per unit mass acting on a particle at a point $\mathbf{r}$ due to the gravitational potential (1) is given by

$$F(\mathbf{r}) = -\nabla U(\mathbf{r})$$

If $\mathbf{r}$ and $\dot{\mathbf{r}}$ are initially in the equatorial plane, then the angular momentum is constant [26], both remain in this plane, and $\phi = 0$. It then follows that in this plane, the specific gravitational force $F(\mathbf{r}) = -f(r)\mathbf{r}$ is central, where

$$f(r) = \mu\left(\frac{1}{r^3} + \frac{3R^2 J_2}{2r^5}\right) \tag{2}$$

In this equatorial plane, the equation of motion of a satellite subject to a central gravitational field and quadratic drag is given therefore by

$$\ddot{\mathbf{r}} = -f(r)\mathbf{r} - \alpha\rho(r)(\dot{\mathbf{r}}\cdot\dot{\mathbf{r}})^{1/2}\dot{\mathbf{r}} \tag{3}$$

where $\rho(r)$ is a model for the atmospheric density and α is a constant that depends on the drag coefficient and the geometry of the satellite. It should be observed that because the motion is confined to the equatorial plane, then Eq. (3) is of the same form as Eq. 1 of [19]. For this reason, the orbit equation is given by Eq. 5 of [19]. To keep this work self-contained, however, we present a brief derivation of this equation.

Received 7 September 2008; revision received 21 April 2009; accepted for publication 21 April 2009.

*Professor of Mathematics, 100 Institute Road; mhumi@wpi.edu.
†Professor Emeritus, Department of Mathematics; cartert@easternct.edu. Senior Member AIAA.

Introducing polar coordinates (r, θ) in the equatorial plane, Eq. (3) becomes

$$r\ddot{\theta} + 2\dot{r}\,\dot{\theta} = -\alpha\rho(r)(\dot{\mathbf{r}}\cdot\dot{\mathbf{r}})^{1/2}r\dot{\theta} \tag{4}$$

$$\ddot{r} - r\dot{\theta}^2 = -\frac{\mu}{r^2} - \frac{\mu k}{r^4} - \alpha\rho(r)(\dot{\mathbf{r}}\cdot\dot{\mathbf{r}})^{1/2}r\dot{\theta} \tag{5}$$

where $k = \frac{3}{2}R^2 J_2$. Multiplying Eq. (4) by r and integrating, it follows that

$$J = r^2\dot{\theta} = h\exp\left(-\alpha\int\rho(r)(\dot{\mathbf{r}}\cdot\dot{\mathbf{r}})^{1/2}\mathrm{d}t\right) \tag{6}$$

where h is a constant of integration that represents the initial value of J. If θ_1 denotes the initial value of θ, then $h = r(\theta_1)^2\dot{\theta}(\theta_1)$. When the tangential velocity of the satellite is much larger than the radial velocity (viz, $\dot{r} \ll r\dot{\theta}$) the expression for J can be approximated by [14]

$$J = h\exp\left(-\alpha\int\rho(r)r\mathrm{d}\theta\right) \tag{7}$$

Using the fact that

$$\frac{d}{dt} = \frac{J}{r^2}\frac{d}{d\theta} \tag{8}$$

and, from Eq. (7),

$$\frac{dJ}{d\theta} = -\alpha\rho(r)rJ \tag{9}$$

we obtain from Eq. (5) and some algebra the following orbit equation for the radial distance r as a function of θ:

$$\frac{r''}{r} - 2\left(\frac{r'}{r}\right)^2 = 1 - \frac{\mu}{J^2}\left(r + \frac{k}{r}\right) \tag{10}$$

Here, primes denote differentiation with respect to θ.

III. Local Solution of the Orbit Equation

Assuming that the radial distance r of the satellite orbit is in the vicinity of R_0, we introduce a new variable $u(\theta)$ so that

$$r = R_0 e^{2u}, \qquad |u| \ll 1 \tag{11}$$

Substituting into Eq. (10), we obtain

$$2u'' = 1 - \frac{\mu}{J^2}\left(R_0 e^{2u} + \frac{k}{R_0}e^{-2u}\right) \tag{12}$$

A. Local Approximation of the Atmospheric Density Function

When the atmospheric density can be approximated locally around R_0 by k_1/r, where k_1 is a constant, expression (7) for J yields

$$J = he^{-\alpha k_1(\theta-\theta_1)} \tag{13}$$

where θ_1 is the initial value of θ. Equation (12) becomes

$$2u'' = 1 - \frac{\mu}{h^2}e^{2\alpha k_1(\theta-\theta_1)}\left(R_0 e^{2u} + \frac{k}{R_0}e^{-2u}\right) \tag{14}$$

Combining the exponentials on the right-hand side of this equation and using the fact that $\alpha \ll 1$ and $|u| \ll 1$, we can approximate this equation by

$$2u'' = 1 - \frac{\mu}{h^2}\Bigg(R_0[1 + 2u + 2\alpha k_1(\theta-\theta_1)] + \frac{k}{R_0}[1 - 2u + 2\alpha k_1(\theta-\theta_1)]\Bigg) \tag{15}$$

Rearranging terms and simplifying, this can be expressed in the form

$$u'' + b_1 u = \frac{1-\beta}{2} - \alpha\beta k_1(\theta-\theta_1) \tag{16}$$

where

$$b_1 = \frac{\mu}{h^2}\left(R_0 - \frac{k}{R_0}\right) \tag{17}$$

and

$$\beta = \frac{\mu}{h^2}\left(R_0 + \frac{k}{R_0}\right) \tag{18}$$

The general solution of this second-order linear differential equation is straightforward:

$$u = C_1\cos\nu(\theta-\theta_1) + C_2\sin\nu(\theta-\theta_1) + \frac{1-\beta}{2\nu^2} - \frac{\alpha\beta k_1}{\nu^2}(\theta-\theta_1) \tag{19}$$

where

$$\nu = \sqrt{b_1} \tag{20}$$

and by differentiation,

$$u' = -C_1\nu\sin\nu(\theta-\theta_1) + C_2\nu\cos\nu(\theta-\theta_1) - \frac{\alpha\beta k_1}{\nu^2} \tag{21}$$

From Eq. (11), we have

$$r(\theta) \cong R_0(1 + 2u(\theta)), \qquad r'(\theta) = 2r(\theta)u'(\theta) \tag{22}$$

leading to the initial conditions

$$u(\theta_1) = \frac{1}{2}\left(\frac{r(\theta_1)}{R_0} - 1\right), \qquad u'(\theta_1) = \frac{r'(\theta_1)}{r(\theta_1)} \tag{23}$$

The arbitrary constants are readily found in terms of these initial conditions:

$$C_1 = \frac{1}{2}\left(\frac{r(\theta_1)}{R_0} - 1\right) + \frac{\beta-1}{2\nu^2}, \qquad C_2 = \frac{r'(\theta_1)}{2\nu r(\theta_1)} + \frac{\alpha\beta k_1}{\nu^3} \tag{24}$$

We recall from Eq. (6) that

$$h = r(\theta_1)^2\dot{\theta}(\theta_1) \tag{25}$$

For the important special case in which $r(\theta_1) = R_0$ and $r'(\theta_1) = 0$, these simplify:

$$C_1 = \frac{\beta-1}{2\nu^2}, \qquad C_2 = \frac{\alpha\beta k_1}{\nu^3} \tag{26}$$

Having determined the arbitrary constants, the approximate trajectory follows from Eq. (22) as long as $r(\theta)$ remains close enough to R_0 and $r'(\theta)$ to $r'(\theta_1)$ that the linearizations presented previously are sufficiently accurate.

B. More Accurate Local Atmospheric Density Function

In [15] we demonstrated that for a spherical Earth, the two-parameter function

$$\rho = \frac{k_1}{r - c} \tag{27}$$

provides a more accurate approximation of the atmospheric density data. The value of the parameter c is determined by curve-fitting procedures (e.g., method of least squares). Applying this density model to the present problem, expression (7) for J becomes

$$J = he^{-\alpha \int \frac{r d\theta}{r-c}} \tag{28}$$

where the constant α has been redefined, absorbing the constant k_1. Again, the problem is to accurately approximate J in a way that yields a closed-form solution. As in the previous work [15], we can write

$$\frac{r}{r-c} = \frac{1}{1-c/r} \tag{29}$$

but c/r is not small enough to gain an accurate approximation by direct linearization. Again, as in the previous work, we let δ be a small positive number that is greater than and near $1 - c/R$ and then write

$$\frac{1}{1-c/r} = \frac{1}{\delta}\left[1\bigg/\left(1 - \frac{\delta - (1-c/r)}{\delta}\right)\right] \tag{30}$$

Because

$$\left|\frac{\delta - (1-c/r)}{\delta}\right| \ll 1$$

the right-hand side of Eq. (30) is linearized by

$$\frac{1}{\delta}\left[1 + \frac{\delta - (1-c/r)}{\delta}\right] = \frac{2\delta - 1}{\delta^2} + \frac{c/r}{\delta^2} \tag{31}$$

Using Eq. (11), this leads to the approximation

$$\frac{r}{r-c} \cong \frac{2\delta - 1}{\delta^2} + \frac{ce^{-2u}}{R_0\delta^2} \tag{32}$$

Because $|u| \ll 1$, this can be approximated by the formula

$$\frac{r}{r-c} = \frac{2\delta + c/R_0 - 1}{\delta^2} - \frac{2cu}{R_0\delta^2} \tag{33}$$

As in [15], we introduce the variable

$$w = \int u(\theta) d\theta \tag{34}$$

where $w(\theta_1) = 0$. The approximate expression for J becomes

$$J = he^{-\alpha[K(\theta-\theta_1) + \frac{2c}{R_0\delta^2}w]} \tag{35}$$

where

$$K = \frac{2\delta + c/R_0 - 1}{\delta^2} \tag{36}$$

Because $\alpha \ll 1$, we linearize the right-hand side of Eq. (35). Because $|u| \ll 1$, we also linearize the right-hand side of Eq. (12) as in the previous example. Because $w' = u$, the linearized orbit equation becomes

$$w''' + b_1 w' + b_2 w = \frac{1-\beta}{2} - \alpha\beta K(\theta - \theta_1) \tag{37}$$

where b_1 and β are again defined, respectively, by Eqs. (17) and (18) and

$$b_2 = \frac{2\alpha\beta c}{\delta^2 R_0} \tag{38}$$

This is the linearized orbit equation with the atmospheric density approximated by Eq. (27)

C. More Elegant Local Atmospheric Density Function

Recently, another formula for representation of the atmospheric density in the vicinity of R_0 has appeared [16]:

$$\rho(r) = \frac{k_1}{r} + \frac{k_2}{r^2} \tag{39}$$

The constants k_1 and k_2 are determined from actual atmospheric density data near R_0 by simple curve-fitting methods. The formula was highly effective in establishing closed-form solutions of the orbit equation under the assumption of a spherical central body and a low ratio of radial to tangential speeds.

For the present problem of equatorial orbits about an oblate body and a low ratio of radial to tangential speeds, the expression for J becomes

$$J = h\exp\left\{-\alpha\left[k_1(\theta - \theta_1) + \frac{k_2}{R_0}\int e^{-2u} d\theta\right]\right\} \tag{40}$$

where, again, θ_1 is the initial value of θ.

Because r is in the vicinity of R_0, then $|u| \ll 1$, and we can again approximate the expression e^{-2u} by the expression $1 - 2u$, then J can be approximated by

$$J = h\exp\left\{-\alpha\left[\left(k_1 + \frac{k_2}{R_0}\right)(\theta - \theta_1) - \frac{2k_2}{R_0}w\right]\right\} \tag{41}$$

and

$$w' = u, \qquad w(\theta_1) = 0 \tag{42}$$

Substituting Eq. (41) into the transformed orbit Eq. (12), we obtain

$$\begin{aligned} 2u'' = 1 &- \frac{\mu R_0}{h^2}\exp\left\{2u + 2\alpha\left[\left(k_1 + \frac{k_2}{R_0}\right)(\theta - \theta_1) - \frac{2k_2}{R_0}w\right]\right\} \\ &- \frac{\mu k}{h^2 R_0}\exp\left\{-2u + 2\alpha\left[\left(k_1 + \frac{k_2}{R_0}\right)(\theta - \theta_1) - \frac{2k_2}{R_0}w\right]\right\} \end{aligned} \tag{43}$$

Using the facts that $|u| \ll 1$ and $\alpha \ll 1$, we linearize this equation, approximating it by

$$2u'' = 1 - \beta - 2b_1 u - 2\alpha\beta K(\theta - \theta_1) + 4\frac{\alpha\beta k_2}{R_0}w \tag{44}$$

where b_1 is defined in Eq. (17) and β is defined in Eq. (18), and, for this case,

$$K = k_1 + \frac{k_2}{R_0} \tag{45}$$

We observe that if $k_2 = 0$, this equation reduces to Eq. (15). We therefore assume from this point on that $k_2 \neq 0$.

Using Eqs. (42) with Eq. (44), we arrive at the following linear differential equation:

$$w''' + b_1 w' + b_2 w = \frac{1-\beta}{2} - \alpha\beta K(\theta - \theta_1) \tag{46}$$

where, in this case,

$$b_2 = -\frac{2\alpha\beta k_2}{R_0} \tag{47}$$

We observe that although the constants b_2 and K are different, this is the same differential equation as Eq. (37).

D. Solution of the Linear Differential Equation

Because r is in the vicinity of R_0, the approximation (22) applies and the initial conditions are determined from Eqs. (23) and (42); the initial specific angular momentum is given by Eq. (25).

The homogeneous form of Eq. (46) or Eq. (37) has the associated characteristic equation:

$$\lambda^3 + b_1\lambda + b_2 = 0 \tag{48}$$

This cubic equation has a real root

$$\lambda_1 = \frac{a}{6} - \frac{2b_1}{a} \tag{49}$$

where

$$a = (-108b_2 + 12\sqrt{12b_1^3 + 81b_2^2})^{1/3} \tag{50}$$

and a complex conjugate pair of roots

$$\lambda_{2,3} = \sigma \pm i\omega \tag{51}$$

where

$$\sigma = -\frac{a}{12} + \frac{b_1}{a}, \qquad \omega = \frac{\sqrt{3}}{2}\left(\frac{a}{6} + \frac{2b_1}{a}\right) \tag{52}$$

It is straightforward to find the complete solution of Eq. (46) in terms of arbitrary constants c_1, c_2, and c_3. By differentiating, we also obtain u and u'. We list these general solutions:

$$w = c_1 e^{\lambda_1(\theta-\theta_1)} + e^{-\frac{\lambda_1}{2}(\theta-\theta_1)}[c_2 \sin\omega(\theta-\theta_1) + c_3\cos\omega(\theta-\theta_1)] + A + B(\theta-\theta_1) \tag{53}$$

$$u = \lambda_1 c_1 e^{\lambda_1(\theta-\theta_1)} + e^{-\frac{\lambda_1}{2}(\theta-\theta_1)}\left[-\left(\frac{\lambda_1}{2}c_2 + \omega c_3\right)\sin\omega(\theta-\theta_1) + \left(\omega c_2 - \frac{\lambda_1}{2}c_3\right)\cos\omega(\theta-\theta_1)\right] + B \tag{54}$$

$$u' = \lambda_1^2 c_1 e^{\lambda_1(\theta-\theta_1)} + e^{-\frac{\lambda_1}{2}(\theta-\theta_1)}\left\{\left[\left(\frac{\lambda_1^2}{4} - \omega^2\right)c_2 + \lambda_1\omega c_3\right] \times \sin\omega(\theta-\theta_1) + \left[-\lambda_1\omega c_2 + \left(\frac{\lambda_1^2}{4} - \omega^2\right)c_3\right]\cos\omega(\theta-\theta_1)\right\} \tag{55}$$

where

$$A = \frac{1-\beta}{2b_2} + \frac{\alpha\beta b_1}{b_2}K \tag{56}$$

and

$$B = -\alpha\beta K \tag{57}$$

To solve the initial value problem, we set $\theta = \theta_1$ in these equations and apply the initial conditions, obtaining

$$c_1 + c_3 = -A \tag{58}$$

$$\lambda_1 c_1 + \omega c_2 - \frac{\lambda_1}{2}c_3 = P \tag{59}$$

$$\lambda_1^2 c_1 - \lambda_1\omega c_2 + \left(\frac{\lambda_1^2}{4} - \omega^2\right)c_3 = P_1 \tag{60}$$

where

$$P = \frac{1}{2}\left[\frac{r(\theta_1)}{R_0} - 1\right] - B, \qquad P_1 = \frac{1}{2}\frac{r'(\theta_1)}{r(\theta_1)} \tag{61}$$

The solution of the linear system (58–60) is straightforward:

$$c_1 = \frac{-(\lambda_1^2 + 4\omega^2)A + 4\lambda_1 P + 4P_1}{9\lambda_1^2 + 4\omega^2} \tag{62}$$

$$c_2 = \frac{\lambda_1(4\omega^2 - 3\lambda_1^2)A + (4\omega^2 + 3\lambda_1^2)P - 6\lambda_1 P_1}{\omega(9\lambda_1^2 + 4\omega^2)} \tag{63}$$

$$c_3 = -\frac{8\lambda_1^2 A + 4\lambda_1 P + 4P_1}{9\lambda_1^2 + 4\omega^2} \tag{64}$$

Having $u(\theta)$ from Eq. (54), we obtain $r(\theta)$ and $r'(\theta)$ from Eq. (22), where u' is found from Eq. (55). Finally, from the chain rule, we get

$$\dot{r}(\theta) = \frac{2hu'(\theta)}{r(\theta)} \tag{65}$$

In calculating P_1, we use the fact that $r'(\theta_1) = \dot{r}(\theta_1)/\dot{\theta}(\theta_1) = \dot{r}(\theta_1)r^2(\theta_1)/h$.

E. Special Cases

We now consider certain simplifications that occur in special cases.

1. *Spherical Planet with Drag*

For a spherical body, $J_2 = 0$; consequently, $k = 0$ in the preceding equations. The result is that

$$b_1 = \beta = \frac{\mu R_0}{h^2} \tag{66}$$

Equations (53–55) and Eqs. (62–65) provide an alternative to the equations presented in [19] for this problem.

2. *Equatorial Orbit About an Oblate Planet Without Drag*

If $\alpha = 0$, Eq. (44) simplifies to

$$u'' + b_1 u = \tfrac{1}{2}(1-\beta) \tag{67}$$

The general solution of this differential equation is

$$u = C_1 \sin\sqrt{b_1}(\theta-\theta_1) + C_2\cos\sqrt{b_1}(\theta-\theta_1) + \frac{1-\beta}{2b_1} \tag{68}$$

Differentiating this expression, then setting $\theta = \theta_1$, we solve for the constants in terms of the initial conditions and get

$$C_1 = \frac{r'(\theta_1)}{2\sqrt{b_1}r(\theta_1)}, \qquad C_2 = \frac{r(\theta_1)}{2R_0} - \frac{1}{2b_1}(1 + b_1 - \beta) \tag{69}$$

We obtain $r(\theta)$ and $r'(\theta)$ from the expressions (22). The resulting formula for $r(\theta)$ is

$$r = 2R_0[C_1\sin\sqrt{b_1}(\theta-\theta_1) + C_2\cos\sqrt{b_1}(\theta-\theta_1)] + \frac{R_0}{b_1}(1 + b_1 - \beta) \tag{70}$$

This equation shows that small deviations from a circular orbit are approximately sinusoidal.

One should observe from Eq. (70) that if the orbit is circular of radius R_0, then $\beta = 1$. It follows from Eq. (17) that the radius of the circular orbit satisfies the equation

$$R_0^2 - \frac{h^2}{\mu}R_0 + k = 0 \tag{71}$$

This is identical to the expression derived in [23] for a circular orbit about an oblate spheroid.

3. *Spherical Planet Without Drag*

If $J_2 = 0$ and $\alpha = 0$, we can apply Eqs. (66–70) and obtain

$$r = 2R_0[C_1\sin\sqrt{b_1}(\theta-\theta_1) + C_2\cos\sqrt{b_1}(\theta-\theta_1)] + \frac{h^2}{\mu} \tag{72}$$

It is well known that $R_0 = h^2/\mu$ for a circular orbit of radius R_0.

F. Analytical Solutions for $u(\theta)$ with Implicit $\rho(r)$

In Sec. III.A, the one-parameter approximation of the atmospheric density function led to a second-order linear differential equation that approximated the flight path. More accurate representations were presented in Secs. III.B and III.C, in which two-parameter approximations of the density function led to third-order linear differential equations. In the following, we attempt to obtain another: a two-parameter approximation of the density function that leads to a second-order differential equation. As we shall see, we pay for this novel approach by having to solve a set of two nonlinear equations.

1. *Differential Equation*

In this approach, we start by making the ansatz:

$$\rho(r) = \frac{1}{r}\left(k_1 + k_2 \frac{du}{d\theta}\right) \tag{73}$$

where k_1 and k_2 are parameters. With this ansatz, the expression (7) for J becomes

$$J = he^{-\alpha[k_1(\theta-\theta_1)+k_2 u]} \tag{74}$$

Again, θ_1 denotes the initial value of θ and there is no loss of generality by setting $u(\theta_1) = 0$. The differential equation (12) for u becomes

$$2u'' = 1 - \frac{\mu}{h^2} e^{2\alpha[k_1(\theta-\theta_1)+k_2 u]}\left(R_0 e^{2u} + \frac{k}{R_0} e^{-2u}\right) \tag{75}$$

Combining the exponentials on the right-hand side of this equation and using the fact that $\alpha \ll 1$ and $|u| \ll 1$, we can approximate this equation by

$$\begin{aligned} 2u'' = 1 &- \frac{\mu R_0}{h^2}[1 + 2\alpha k_1(\theta - \theta_1) + 2(\alpha k_2 + 1)u] \\ &- \frac{\mu k}{h^2 R_0}[1 + 2\alpha k_1(\theta - \theta_1) + 2(\alpha k_2 - 1)u] \end{aligned} \tag{76}$$

Rearranging and simplifying, we arrive at the following second-order linear differential equation:

$$u'' + (b_1 + \alpha\beta k_2)u = \frac{1-\beta}{2} - \alpha\beta k_1(\theta - \theta_1) \tag{77}$$

where b_1 and β are the ubiquitous constants first defined in Eqs. (17) and (18). A comparison of this equation with Eq. (16) is inevitable. If we set

$$\nu = (b_1 + \alpha\beta k_2)^{1/2} \tag{78}$$

the form of the general solution is given by Eq. (19) and its derivative is given by Eq. (21). The arbitrary constants are determined from the initial conditions by the formulas (24)

2. *Solving a Problem*

To solve an actual problem, we must pick the parameters k_1 and k_2 so that along the trajectory that results, the function (73) closely approximates the data points of the actual atmospheric density function. It appears that the simplest way to accomplish this is to pick the atmospheric density data points $\rho(r_1)$ and $\rho(r_2)$ so that r_2 is reasonably close to r_1. It follows from the continuity of the actual density function and approximation (73) that this approximation improves in the limit as r_2 approaches r_1. Setting $r_2 < r_1$ and in the vicinity of r_1, we attempt to satisfy the initial condition

$$r(\theta_1) = r_1 \tag{79}$$

and the terminal condition

$$r(\theta_2) = r_2 \tag{80}$$

evaluating the expression (73) and Eq. (19) at these boundary conditions. To simplify the notation, we set

$$\phi = \nu(\theta_2 - \theta_1) \tag{81}$$

If we specify r_2, then three constants (k_1, k_2, and ϕ) must satisfy the three equations

$$k_1 + \frac{r'(\theta_1)}{2r_1} k_2 = \rho(r_1) r_1 \tag{82}$$

$$\left(-C_1 \nu \sin\phi + C_2 \nu \cos\phi - \frac{\alpha\beta}{\nu^2} k_1\right) k_2 = \rho(r_2) r_2 - k_1 \tag{83}$$

$$-\frac{\alpha\beta}{\nu^3} k_1 \phi + C_1 \cos\phi + C_2 \sin\phi = \frac{r_2 - R_0}{2R_0} + \frac{\beta - 1}{2\nu^2} \tag{84}$$

where ν depends on k_2, C_1 depends on k_2 through ν, and C_2 depends on k_1 and k_2. One can solve Eq. (82) for k_1 and further reduce these to a system of two equations in k_2 and ϕ.

An alternative problem would be to specify θ_2 and solve the system (82–84) for k_1, k_2, and r_2.

3. *Important Special Case*

An important special case is one in which the initial velocity is tangential at a radial distance R_0 [i.e., $r(\theta_1) = R_0$ and $r'(\theta_1) = 0$]. In this case, Eq. (82) simplifies to

$$k_1 = R_0 \rho(R_0) \tag{85}$$

and the arbitrary constants are specified by Eqs. (26). As a result, Eqs. (83) and (84) reduce to the two equations

$$\begin{aligned} &\frac{1-\beta}{2}\sin\phi - \frac{\alpha\beta R_0 \rho(R_0)}{\nu}(1 - \cos\phi) \\ &\quad = \left(\frac{\alpha\beta\nu}{\nu^2 - b_1}\right)[\rho(r_2) r_2 - R_0 \rho(R_0)] \end{aligned} \tag{86}$$

$$\frac{1-\beta}{2}(1 - \cos\phi) + \frac{\alpha\beta R_0 \rho(R_0)}{\nu}(\sin\phi - \phi) = \frac{\nu^2 (r_2 - R_0)}{2R_0} \tag{87}$$

in the two unknowns ϕ and ν. From the solutions of these two equations, we can calculate k_2 from Eq. (78).

G. Numerical Model Testing

The four closed-form solutions presented herein have been compared with numerical integration of Eqs. (4) and (5), where J is given by Eq. (7) and a test model of the atmospheric density is chosen as

$$\rho = \rho_0 e^{(r-R_0)/H} \tag{88}$$

where ρ_0 is the atmospheric density at R_0. We want to emphasize that this formula is commonly used to model local atmospheric density. The four models presented herein are also applicable to other representations of atmospheric density, even if presented in tabular form such as the U. S. Standard Atmosphere published by the National Oceanic and Atmospheric Administration.

The constants c, k_1, and k_2 found in the four models are calculated from the atmospheric density data by curve-fitting procedures such as the method of least squares. We have found that the atmospheric density is so low for satellite orbits such as those considered in this paper that only two data points are usually sufficient. If not, one can recalibrate the constants in the models by using additional pairs of data points as the orbit decays. This was demonstrated in a previous study [19] and more details can be found therein.

In the computational studies that were performed ($H = 88.667$ km), the atmospheric density was normalized (i.e., $\rho_0 = 1$) and the initial radial distance R_0 was set at 6700 km. In all studies, $J_2 = 0.00108263$, $\alpha = 10^{-11}$, $\theta_1 = 0$, and $r'(0) = 0$ so that the initial velocity was tangential at circular speed. The simulations were

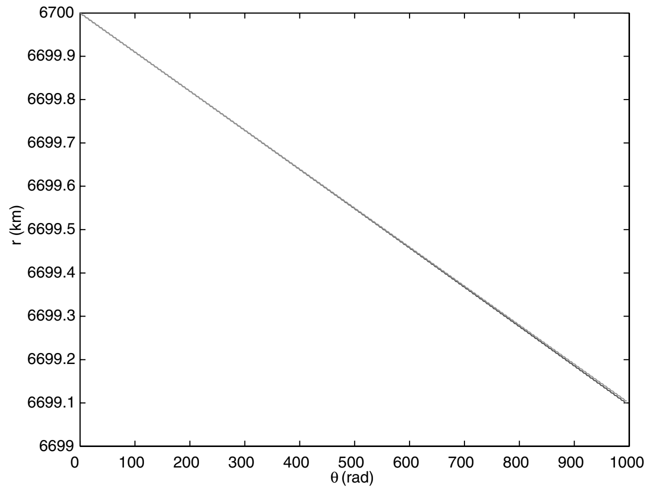

Fig. 1 Flight paths: numerically exact model and k_1/R model.

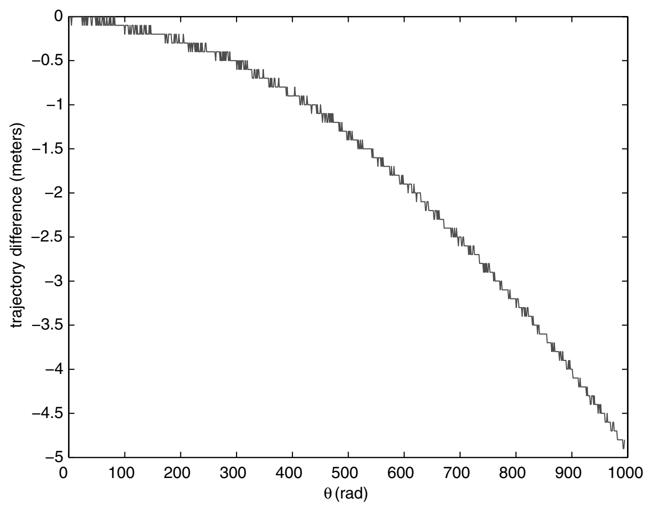

Fig. 2 Difference: numerically exact model and k_1/R model.

carried out for nearly 160 revolutions, which is about 10 days. Each revolution took 90 min. The numerical integration was done using an adaptive-step implicit fourth-order Runge–Kutta method with an absolute error tolerance of 10^{-10}. The results showed a drop of 900 m due to drag as calculated numerically from the equations of motion using the test model for ρ. All of the analytical solutions were comparable, with the worst cases having a maximal error of 5 m.

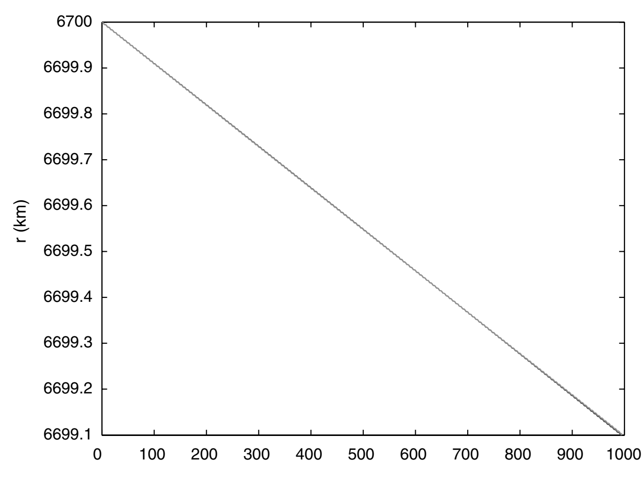

Fig. 3 Flight paths: numerically exact model and $k_1/(R-c)$ model.

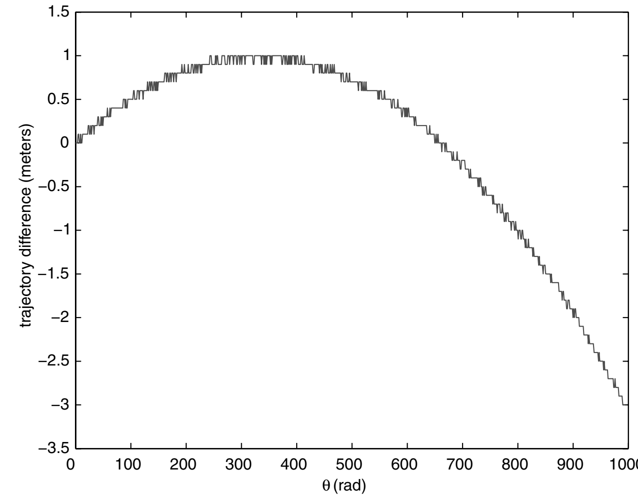

Fig. 4 Difference: numerically exact model and $k_1/(R-c)$ model.

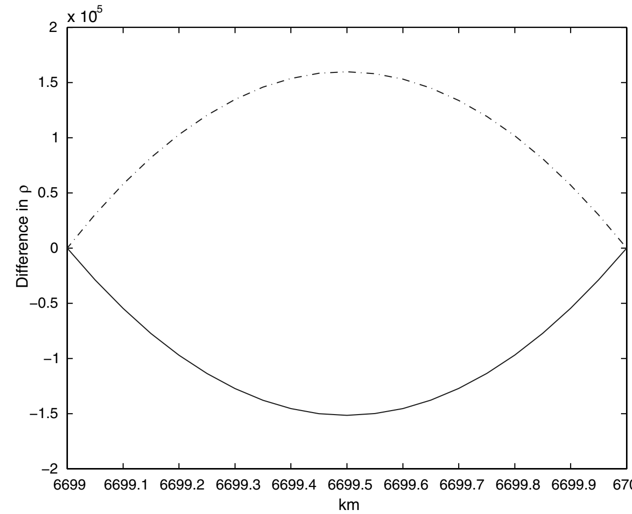

Fig. 5 Differences in ρ: exponential atmosphere and $k_1/R + k_2/R^2$ (solid line) and exponential atmosphere and $k_1/(R-c)$ (dashed line).

1. k_1/r Model

Figure 1 presents a comparison of $r(\theta)$ as calculated from Eq. (19), where $\rho(\theta) = k_1/r$ with a numerical solution of Eqs. (4) and (5), where $\rho(\theta)$ is calculated from Eq. (88). The plot shows very good accuracy of the closed-form solution over 1000 rad (nearly 160 revolutions) of the satellite, during which the atmospheric drag causes

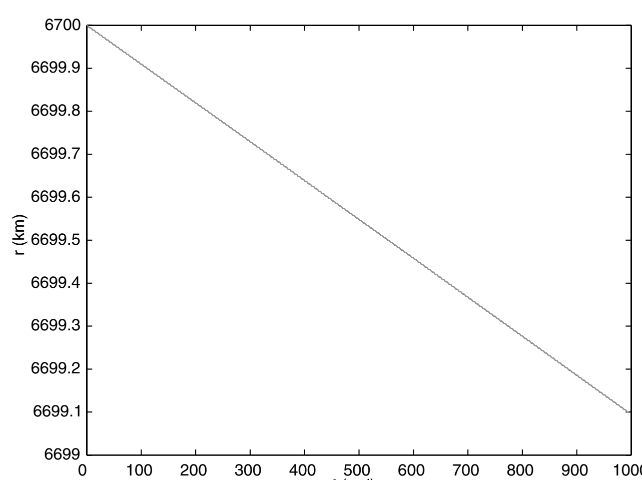

Fig. 6 Flight paths: numerically exact model and $k_1/R + k_2/R^2$ model.

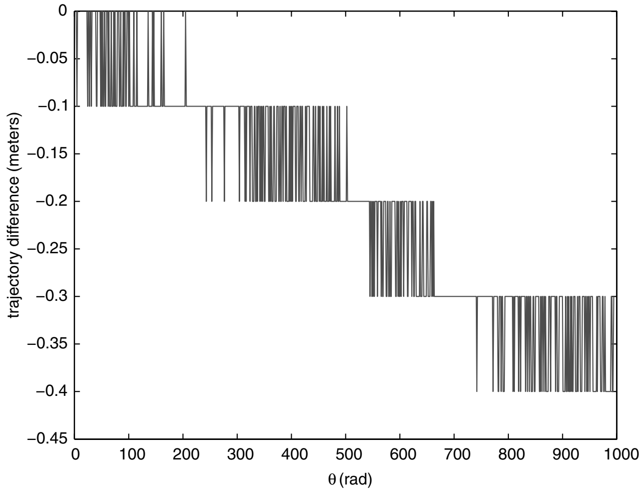

Fig. 7 Difference: numerically exact model and $k_1/R + k_2/R^2$ model.

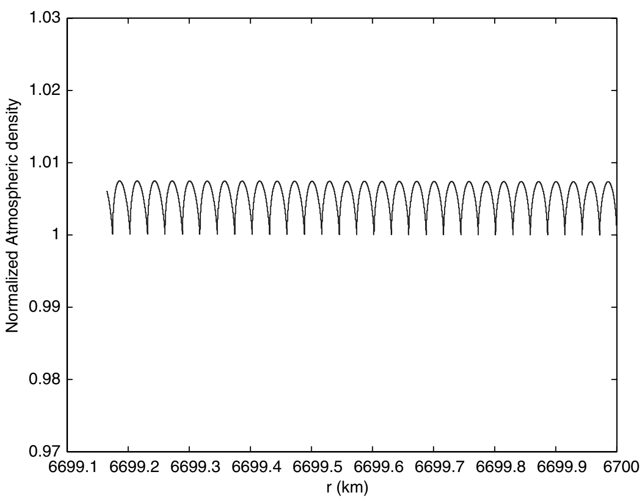

Fig. 8 Implicit model: normalized atmospheric density as a function of height.

a loss in altitude of about 900 m. As seen from Fig. 2, the error in the closed-form solution is about 5 m near the end of 160 revolutions, but the magnitude of the rate of error is increasing and wider divergence between the two curves is expected beyond 160 revolutions.

2. $k_1/(r-c)$ Model

In this model, the constants k_1 and c were chosen to fit the curve defined by Eq. (88) over a drop of altitude of 900 m. The numerical

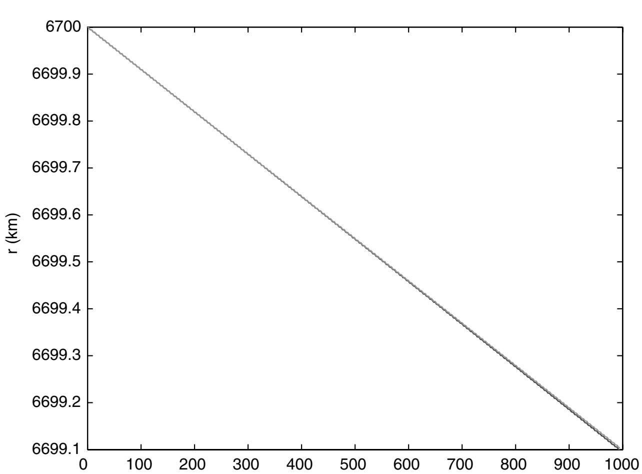

Fig. 9 Flight paths: numerically exact model and implicit ρ model.

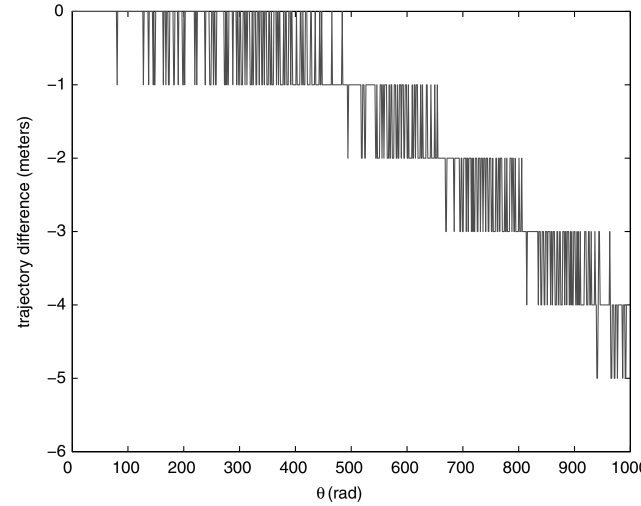

Fig. 10 Difference: numerically exact model and implicit ρ model.

and closed-form solutions for $r(\theta)$ over a duration of almost 160 revolutions are presented in Fig. 3. The error in the closed-form solution is depicted in Fig. 4. This figure shows a maximum error of about 3 m over 1000 rad and is an improvement over the previous model.

A source of much of the error from this model lies in the selection of the parameter δ introduced in Eq. (30). The subsequent model that we will present will be seen to be much more accurate in $r(\theta)$, but about the same level of accuracy in $\rho(\theta)$, as can be seen from Fig. 5.

3. $k_1/r + k_2/r^2$ Model

This is the most accurate model of the four. The two plots presented in Fig. 6 are indistinguishable to the eye. The error in this closed-form solution is only 0.4 m and is not increasing at the end of 1000 rad, as shown in Fig. 7.

4. Implicit ρ Model

This model was selected for its novelty. It calculates an approximate atmospheric density model simultaneously with the flight path. A plot of the calculated density model is presented in Fig. 8. The curve should be viewed as very-low-amplitude oscillations about an atmospheric density $\rho(\theta)$. A plot of this closed-form solution with the numerical solution is presented in Fig. 9. An accuracy of about 5 m is seen from Fig. 10 and is comparable with the first two models.

IV. Conclusions

We have presented four atmospheric density models that can be used to approximate local atmospheric density data and that lead to closed-form solution of the flight path of a satellite near a circular equatorial orbit. All of the models produced an accuracy within 5 m over a duration of about 10 days when compared with numerical integration using test atmospheric data at an initial radial distance of 6700 km and a degradation of altitude of 900 m. The first model, which is the simplest, was the least accurate. The third model, however, was found to be the most accurate, having an error of only 0.4 m over a duration of 160 revolutions.

This has been an introductory study. All the simulations were based on the degradation of an orbit that was initially circular. There is a need for more simulations over a wider range of conditions. All the models should provide much better accuracy under more realistic orbits that are subject to lower levels of atmospheric drag. Higher levels of atmospheric drag or much longer flight durations can be approached by reinitialization of the parameters of the closed-form solutions.

References

[1] King-Hele, D., and Merson, R. H., "Satellite Orbits in Theory and Practice," *Journal of the British Interplanetary Society*, Vol. 16, No. 8, 1958, pp. 446–471.

[2] Clohessy, W. H., and Wiltshire, R. S., "Terminal Guidance System for Satellite Rendezvous," *Journal of the Aerospace Sciences*, Vol. 27, No. 9, 1960, pp. 653–658.

[3] Lawden, D. F., *Optimal Trajectories for Space Navigation*, Butterworths, London, 1963.

[4] Tschauner, J., and Hempel, P., "Rendezvous zu ein Elliptischer Bahn Umlaufenden Ziel," *Astronautica Acta*, Vol. 11, 1965, pp. 104–109.

[5] Burns, J. A., "Elementary Derivation of the Perturbation Equations in Celestial Mechanics," *American Journal of Physics*, Vol. 44, No. 10, 1976, pp. 944–949.
doi:10.1119/1.10237

[6] King-Hele, D., *Satellite Orbits in an Atmosphere*, Blackie, London, 1987.

[7] Carter, T., and Humi, M., "Fuel-Optimal Rendezvous Near a Point in General Keplerian Orbit," *Journal of Guidance, Control, and Dynamics*, Vol. 10, No. 6, 1987, pp. 567–573.

[8] Humi, M., "Fuel-Optimal Rendezvous in a General Central Force Field," *Journal of Guidance, Control, and Dynamics*, Vol. 16, No. 1, 1993, pp. 215–217.
doi:10.2514/3.11448

[9] Carter, T. E., "State-Transition Matrices for Terminal Rendezvous Studies: Brief Survey and New Example," *Journal of Guidance, Control, and Dynamics*, Vol. 21, No. 1, 1998, pp. 148–155.
doi:10.2514/2.4211

[10] Melton, R. G., "Time-Explicit Representation of Relative Motion Between Elliptical Orbits," *Journal of Guidance, Control, and Dynamics*, Vol. 23, No. 4, 2000, pp. 604–610.
doi:10.2514/2.4605

[11] Brouwer, D., and Hori, G., "Theoretical Evaluation of Atmospheric Drag Effects in the Motion of an Artificial Satellite," *Astronomical Journal*, Vol. 66, No. 5, 1961, pp. 193–225.
doi:10.1086/108399

[12] Brouwer, D., and Clemence, G. M., *Methods of Celestial Mechanics*, Academic Press, New York, 1961, pp. 574–582.

[13] Liu, J. J. F., "Advances in Orbit Theory for an Artificial Satellite with Drag," *Journal of the Astronautical Sciences*, Vol. 31, No. 2, 1983, pp. 165–188.

[14] Humi, M., and Carter, T., "Models of Motion in a Central-Force Field with Quadratic Drag," *Celestial Mechanics and Dynamical Astronomy*, Vol. 84, No. 3, 2002, pp. 245–262.
doi:10.1023/A:1020315310491

[15] Carter, T., and Humi, M., "Clohessy-Wiltshire Equations Modified to Include Quadratic Drag," *Journal of Guidance, Control, and Dynamics*, Vol. 25, No. 6, 2002, pp. 1058–1063.
doi:10.2514/2.5010

[16] Humi, M., and Carter, T., "Closed-Form Solutions for Near-Circular Arcs with Quadratic Drag," *Journal of Guidance, Control, and Dynamics*, Vol. 30, No. 1, 2007, pp. 248–251.
doi:10.2514/1.21446

[17] Vallado, D. A., *Fundamentals of Astrodynamics and Application*, McGraw–Hill, New York, 1997, Chaps. 2, 10, 11.

[18] Humi, M., and Carter, T., "Two-Body Problem with High Tangential Speeds and Quadratic Drag," *Journal of Guidance, Control, and Dynamics*, Vol. 30, No. 1, 2007, pp. 248–251.
doi:10.2514/1.21446

[19] Carter, T., and Humi, M., "Two-Body Problem with Drag and High Tangential Speeds," *Journal of Guidance, Control, and Dynamics*, Vol. 31, No. 3, 2008, pp. 641–646.
doi:10.2514/1.31482

[20] Kechichian, J. A., "Motion in General Elliptic Orbit with Respect to a Dragging and Precessing Coordinate Frame," *Journal of the Astronautical Sciences*, Vol. 46, No. 1, 1998, pp. 25–45.

[21] Gim, D. W., and Alfriend, K. T., "State Transition Matrix of Relative Motion for the Perturbed Non-Circular Reference Orbit," *Journal of Guidance, Control, and Dynamics*, Vol. 26, No. 6, 2003, pp. 956–971.
doi:10.2514/2.6924

[22] Schweighart, S. A., and Sedwick, R. J., "High-Fidelity Linearized J_2 Model for Satellite Formation Flight," *Journal of Guidance, Control, and Dynamics*, Vol. 25, No. 6, 2002, pp. 1073–1080.
doi:10.2514/2.4986

[23] Schweighart, S. A., and Sedwick, R. J., "Cross-Track Motion of Satellite Formations in the Presence of J_2 Disturbances," *Journal of Guidance, Control, and Dynamics*, Vol. 28, No. 4, 2005, pp. 824–826.
doi:10.2514/1.12387

[24] Breger, L., How, J. P., and Alfriend, K. T., "Maneuver-Optimized J_2-Invariant Initial Conditions," *Flight Mechanics Symposium*, CP-2005-212789, NASA Goddard Space Flight Center, Greenbelt, MD, 18–20 Oct. 2005.

[25] Humi, M., "The J_2 Effect in Cylindrical Coordinates," *Journal of Guidance, Control, and Dynamics*, Vol. 30, No. 1, 2007, pp. 263–266.
doi:10.2514/1.22517

[26] Humi, M., and Carter, T., "Orbits and Relative Motion in the Gravitational Field of an Oblate Body," *Journal of Guidance, Control, and Dynamics*, Vol. 31, No. 3, 2008, pp. 522–532.
doi:10.2514/1.32413